Journal of Thermal Analysis and Calorimetry, Vol. 95 (2009) 1, 63–68

OXIDATION BEHAVIOUR OF PRECIPITATION HARDENED STEEL TG, X-Ray, XRD and SEM study

G. Vourlias, N. Pistofidis, E. Pavlidou and K. Chrissafis *

Department of Physics, Aristotle University of Thessaloniki, 541 24 Thessaloniki, Greece

In the present work the oxidation behavior of ageing treated steel was examined up to 1000°C in different environments (O_2 and CO_2) and with different heating rates. The examination was conducted by means of thermogravimetric analysis, scanning electron microscopy and X-ray diffraction. In this study it was deduced that in the case of O_2 an oxide scale is formed on top of the steel. The oxidation is uniform and the growth of the scale is more intent at low heating rate. It consist of different Fe, Mn, Mo and Cr oxides which are adjusted in the form of layers. This phenomenon was explained by the different diffusion coefficients of each metal in the already formed scale. Regarding the oxidation in CO_2, the scale formation takes place at a lower temperature than in the case of O_2. Hence the examined substrate is more vulnerable in CO_2.

Keywords: *oxidation, scanning electron microscopy (SEM), steel, TG, X-ray diffraction (XRD)*

Introduction

Stainless steels are iron-base alloys that do not form rust in unpolluted atmospheres [1–3]. This property is developed by the addition of a minimum of approximately 1.1% Cr [4–7], which forms an invisible and adherent chromium-rich oxide surface film that isolates the substrate from its environment. As a matter of fact, the Cr oxide film is so stable that, even in the case of rupture, it heals itself in the presence of oxygen.

A rather new development in the stainless steel industry is the production of precipitation hardened (PH) steels [8]. These materials are characterized by a very important advantage. Although after precipitation they combine high mechanical strength, superficial hardness and stiffness, they can be easily machined to the desirable form before precipitation, while they are still ductile. As a result, they are suitable for the construction of complicated forms, such as injection moulds for plastics and rubber.

The composition of a special type of PH-stainless steel is presented in Table 1. Its oxidation resistance at high temperatures is still unexplored, although its composition implies that it has the ability to form protective superficial oxide scales. If we take into account the fact that chromium and molybdenum increase tensile and creep-rupture strength at high temperatures [9–11], increased oxidation resistance would largely expand the application field of this steel.

Table 1 Typical analysis of the examined steel

Element	C	Si	Mn	Cr	Mo	Al
mass%	0.03	0.3	6.3	12.0	1.4	1.6

For this reason, in the present work the oxidation behavior of the ageing treated form of this steel was examined up to 1000°C in different environments (O_2 and CO_2). For O_2 two different heating rates were applied. The temperature boundary was set because when this limit is exceeded, the microstructure of the alloy changes as solution of the precipitated phases takes place and consequently the mechanical strength is decreased.

The experiments were accomplished in pure gases instead of atmospheric air (which is the usual working environment for this kind of steel) in order to isolate the effect of each gas and determine whether one of these environments is more aggressive with regard to the others. When gaseous reactions involve several active gases (such as O_2, CO_2, SO_2, N_2 etc.), special considerations of competitive product stabilities and growth rates must be considered and as a result the study becomes very complicated.

Experimental

The substrates used were machined in rectangular specimens with dimensions 5×3×2 mm^3, while their surface was very well polished up to 5 μm alumina emulsion. Their oxidation took place in a TG-DTA Setaram Setsys 16/18 in alumina crucibles in O_2 and CO_2 atmosphere with a 50 mL min^{-1} gas flow. Two

* Author for correspondence: hrisafis@physics.auth.gr

1388–6150/$20.00

Akadémiai Kiadó, Budapest, Hungary
Springer, Dordrecht, The Netherlands

different heating rates were used in the case of O_2, that is 1 and 10°C min^{-1} respectively, from ambient temperature up to 1000°C, while in the case of CO_2 the heating rate was only 10°C min^{-1}. TG-DTA allowed also the quantitave estimation of oxidation, while the continuous recording of mass, temperature and time allowed the on-line monitoring of the oxidation phenomena.

The morphology and the chemical composition of the oxidation products were determined with scanning electron microscopy (SEM) using a 20 kV JEOL 840A SEM equipped with an Oxford ISIS 300 EDS analyzer. For the SEM examination, the surface of the samples did not undergo any preparation, while for the examination of the cross-section, segments have been cut from each sample, mounted in bakelite and polished down to 5 μm alumina emulsion.

The structure of the oxidation products was determined with X-ray diffraction. For this purpose, a 2-cycle SEIFERT 3003 TT diffractometer (CuK_α radiation) with Bragg–Brentano geometry was used. To reveal possible structural or compositional variations of the oxidation layer, progressive polishing of the oxidized surface took place, in order to obtain diffraction patterns from different depths. As the scale was very fragile, the oxidized sample was fixed with epoxy resin and the oxide layer was abraded parallel to the surface at about 50 μm at each step with a 2000-grit SiC paper until the substrate was uncovered [12].

Results and discussion

Oxidation in O_2

The oxidation of steel (stainless or not) in oxygen at high temperature is a well known phenomenon [6, 7, 10, 11]. What is rather characteristic is that there is always a combination of environmental and temperature conditions that render the surface of every class of steel vulnerable, although steel composition significantly affects its mechanism, progress and rate [13].

In Fig. 1 the mass change, which refers to heating rates of 1 and 10°C min^{-1}, verifies that over a certain temperature the mass of the sample under examination increases when the measurement takes place in an O_2 atmosphere. Hence, the substrate is oxidized under these circumstances. What is rather characteristic is that in the plot of Fig. 1 there is a certain incubation period. In fact, for heating rate equal to 10°C min^{-1}, two oxidation stages could be distinguished. Up to 900°C the mass increase is very low and the steel surface seems to be rather inert (incubation). However at about 900°C a steep increase begins. The main mass change takes place during this phase. In any case, the appearance of a slope change in the curve implies structural or compositional changes in the scale as the temperature rises, which finally result to its failure. These phenomena will be further examined later with the assistance of SEM and XRD.

Similar results were also observed when the heating rate was 1°C min^{-1}. However, in this case the mass increase was more intense as Fig. 1 shows. The incubation period extends only up to 750°C. The oxidation begins at about 750°C, while at about 850°C a further increase of the oxidation rate is observed. Hence, with this heating rate the oxidation progress is faster. This phenomenon could be explained if we took into account the fact that lower heating rate means longer exposure at every temperature interval. Thus, the available time for reaction was increased and as a result, the mass of the reaction products also increased.

However these measurements do not enlighten the oxidation mechanism. For this reason, the surface of the oxidized samples was initially examined with SEM (Fig. 2). The results observed are characterized by certain similarities regardless the heating rate. In both cases, SEM revealed a dense and adherent scale that although it totally covers the underlying steel, does not exhibit a smooth and regular aspect. This is not peculiar [14]. The boundaries between the different grains of this scale are easily distinguished, while their surface is very rough.

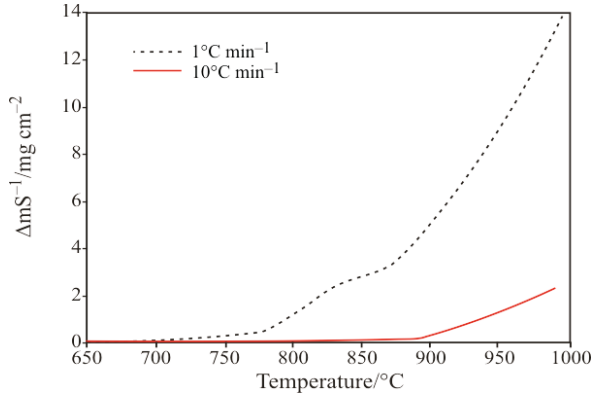

Fig. 1 Thermogravimetric plot of the steel mass change per surface unit *vs*. temperature in O_2 atmosphere with heating rate 1 and 10°C min^{-1}

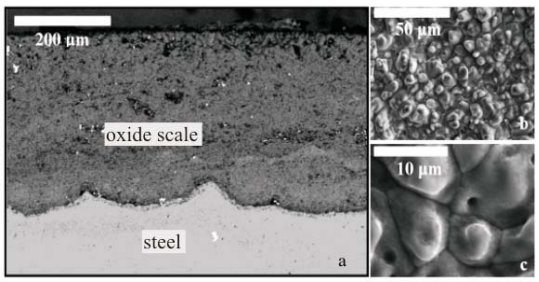

Fig. 2 SEM micrographs of the a – cross-section and the b–c – plane view of oxidized steel after exposure in O_2 atmosphere with heating rate 1°C min^{-1}

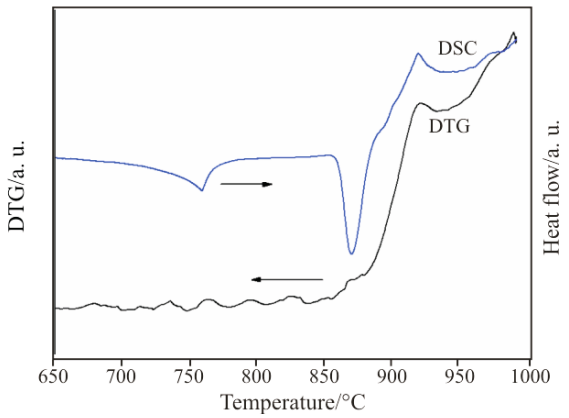

Fig. 3 Heat flow plot along with the plot of its first derivative for the oxidation process after exposure in O_2 atmosphere with heating rate 10°C min^{-1}

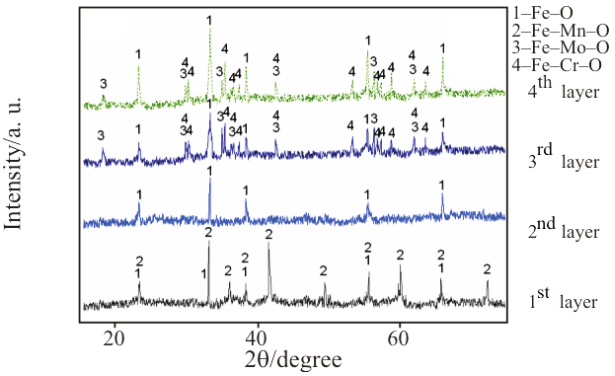

Fig. 4 XRD pattern of the oxidized steel after exposure in O_2 atmosphere (PDF#32-0469, PDF#71-0637, PDF#77-2360, PDF#73-0236, PDF#78-1654, PDF#24-0511, PDF#85-0778 [17])

Nevertheless, a closer look reveals that the scale formed with heating rate 1°C min^{-1} is much thicker. This observation verifies the conclusion drawn by the comparison of the plots of Fig. 1.

Moreover, the scale formed at the lower heating rate is composed by grains that look like small hills with rounded edges. By contrast, the grains of the scale formed at the higher rate are smaller and much rougher, while they have a flower-like aspect instead of the compact appearance of the previous case. Consequently, the evolution of oxidation is affected by the heating rate.

The different grain size could be related to the different exposure at every temperature interval. The lower heating rate favors the growth of the oxide crystals and as a result larger grains are formed.

The different grain appearance could also be explained in a similar way. As the crystal growth is more intense at a lower heating rate, the separate leaves of the flower-like formations are unified and form the rounded hill-like grains.

On the other hand, a different explanation could be proposed based on the fact that at low heating rate the crystals of the scale lack of typical geometrical shapes or sharp edges, as it would be expected in crystal growth phenomena. This observation implies that the grains of the scale melted as the temperature increased, while at higher heating rate this phenomenon did not take place. This opinion is also supported by the presence of round voids of different depth on the surface of several grains, which are very similar to shrinkage voids observed upon solidification of molten materials. Hence it is likely that the crystals of this scale were formed below 1000°C and were liquefied at least superficially as the temperature raised. Nevertheless, a similar phenomenon would be clearly observed in the heat flow plot of the oxidation process (Fig. 3), which is not the fact. In order to verify the existence of different transformations during heating, the heat flow *vs.* temperature was studied. As Fig. 3 shows, the heat flow plot is actually composed of three peaks. The first one (at about 750–770°C) refers to the Curie temperature [15], while the second one to a phase transformation of the ferrous substrate [16]. The third one at 919°C is due to the oxidation of the substrate, as it is also present in the curve referring to the first derivative of the heat flow. Therefore, melting is not likely. Consequently the different appearance is due to the more extensive growth that takes place at a low heating rate. The pores observed in this case are probably the result of incomplete growth of the leaves of the flower-like formations.

More information could be offered by the XRD examination (Fig. 4), which is similar for both coatings, apart from the different thickness of each layer presented in Fig. 5. As it was already mentioned, several diffraction patterns were taken from every sample with progressive grinding of the oxidized surface. In every case different Fe, Mn, Mo and Cr oxides were detected. However, there are differences between the outer and the inner layers. So, the outer layer is mainly composed of Fe and Mn oxides. As the depth increases (and the scale-steel interface is approached) the Mn oxides disappear, while Mo and Cr oxides appear.

The EDS analysis of the scale surface revealed, in both cases, that it is composed of iron, manganese and oxygen.

These compositional variations verified also that the melting of the crystals that was previously discussed did not take place. Indeed, if the scale was melted and solidified again as the temperature dropped, the formation of the liquid phase would have created a homogenized scale and not the layered structure which is examined.

Similar results regarding composition could be drawn by the EDS examination of the cross-section of

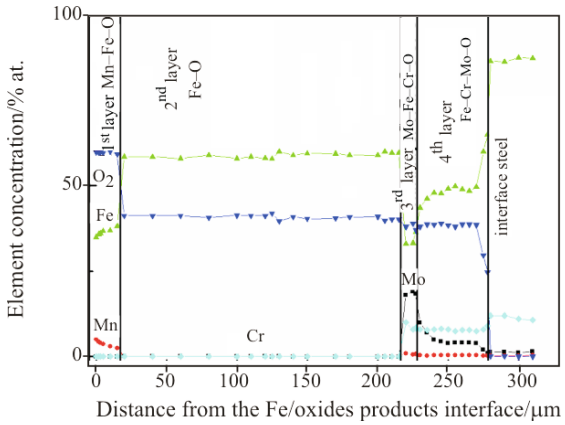

Fig. 5 EDS analysis of the cross-section of the oxidized samples after exposure in O_2 atmosphere with heating rate 1°C min^{-1}

the oxidized samples (Fig. 5). In this case the data is also the same regardless the heating rate (apart from the different thickness of the layers). The cross-section of the samples seems to be composed of different subscales and as a result a multilayered morphology is observed [14]. In each layer different elements are detected. These layers are also possible to be distinguished in the SEM micrographs of the cross-section as we see in Fig. 2. Actually, the Fe–Mn oxides layer (outer) seems to be more porous, while the Fe oxides layer that follows is rather compact. The layer that contains also Mo oxides, which is the thinner one, appears as a thin zone with lighter color. Finally, the layer close to the steel is the most compact.

This diversification of the oxidation products along the cross-section of the scale could be explained with the elementary oxidation theory [10]. Oxidation by gaseous oxygen is an electrochemical process that consists of the metal oxidation at the metal/scale interface and the oxygen reduction at the scale/gas interface. The as-formed ions combine to produce the metal oxide (scale). However, the ion-forming reactions are spatially separated. As a result, the combination of the anions and cations formed from these reactions necessitates their diffusion through the already formed oxide layer (scale). Almost without exception, cations and oxygen anions do not diffuse with comparable ease in a given scale. Thus diffusion control should result in the growth of the scale at either the metal/scale or else the scale/gas interface.

This theory describes oxidation very well when a pure metal is concerned and only one compound is formed. When an alloy is oxidized, as in the case of the examined steel, diffusion of several elements takes place through the scale, while several oxides are formed. As a matter of fact, at equilibrium, all of the potentially stable oxide phases from the metal-oxygen phase diagram would form in sequence, with the most oxygen-rich compound being present at the scale/gas interface. Furthermore, the presence of different elements in the base metal, which are characterized by different diffusivities through the scale and different reactivities, will also enhance the formation of different compounds.

In the case of the steel under examination, the growth of the scale mostly takes place at the scale/gas interface, as it is the fact for the majority of iron alloys [11], although there is also the possibility of the simultaneous action of both mechanisms, where each mechanism is responsible for the formation of different layers of the scale, as it will be explained later [14]. Obviously, the matrix of the scale would be composed of Fe oxides, since Fe is the predominant material in the alloy. However, as far as it concerns the rest of the elements that compose the alloy, it is obvious that the diffusivity of each one would determine its position in the scale and consequently the oxidation front. Hence the scale would be composed of different layers which could be distinguished based on their composition (and probably also on their relief as it is in our case). The elements with higher diffusivity would be detected closer to the gas/scale interface. Following this opinion Fig. 5 implies that Mo has higher diffusivity than Cr, while Mn is the most mobile, since it was enriched in the outer layer [12]. In any case, the presence of Cr oxides at the metal/scale interface is a well known phenomenon [11, 14]. It is caused by the growth of Fe oxides at the scale/gas interface through Fe diffusion, which induces Fe depletion at the scale/steel interface. As a result, Cr enrichment is observed in this area [14].

Furthermore, the high Mn concentration in the outer layer explains the slope change of the mass change curves of Fig. 1. As it was already mentioned, the oxidation resistance of stainless steels is mainly due to the formation of a thin layer of chromia (Cr_2O_3) on their surface. However, Mn diffuses very fast through this layer, leading to its destabilization [18]. Hence, as long as temperature is low, the diffusivity of Mn is low and as a result, chromia is stable and oxidation is not observed under the examined conditions. When temperature reaches a critical value, the protective layer fails and oxidation begins. This phenomenon explains the increase of the oxidation rate which appears as the slope change of the curves.

What is rather peculiar is the pore distribution in the scale. As Fig. 2 shows both scales (regardless the heating rate) seem to be rather compact. However, at their upper part pores and voids appear at much higher density. Furthermore, their size in this area is bigger with regard to the rest of the scale, while cracks are also present. A pore zone is also observed close to the boundary with the high Mo oxides layer.

Nevertheless, in this case their size is much smaller and they are likely to be organized in clusters. Finally, some voids appear also at the scale/substrate interface, but in this area they are rather rare.

The presence of pores and voids in the scale or at the scale/substrate interface could be explained with two mechanisms. First of all, as oxide scales grow, stresses develop, which are mainly due to the differences between the coefficients of linear thermal expansion of the substrate and the oxides of the scale [11]. In polycrystalline oxides, as in the case of the scale under examination, stresses develop along the grain boundaries because of more rapid growth of grains oriented in preferred directions. Furthermore, the compositional variation across the scale also creates stresses. Nevertheless, the cooling from the reaction temperature to ambient has a similar effect. The as-generated stresses tend to relief through the rupture of the scale as it grows. This phenomenon is observed in the form of pores in the scale mass and in some cases in the form of cracks. These cracks are usually gathered close to the boundaries between the oxides of different composition or to the scale/substrate interface.

Apart from the above-described mechanism, in scales that grow at the scale/gas interface the pore formation is also justified by the fast diffusion of metal ions towards the scale surface. This phenomenon is usually limited at the scale/substrate interface or at the other interfaces that exist in the scale. Pores with this origin are not rare in ferrous alloys [10].

In our case it is difficult to discriminate the predominant mechanism for the pore formation. Most probably both mechanisms take place. Furthermore, as it was already mentioned, some subscales might be formed through oxygen inward diffusion (e.g. growth at the scale/substrate interface, where the substrate is a certain oxide) [14]. Hence, in this case the pore formation is not favored, at least at specific interfaces inside the scale. As a result, the situation becomes even more complicated. However, what is important is the fact that the pores are not likely to affect the oxidation resistance of the scale, since they are rather isolated and they do not offer diffusion paths down to the substrate. Consequently, catastrophic oxidation due to this phenomenon is highly improbable.

From the above analysis it seems that oxidation is uniform. Indeed, if oxygen diffused in grain boundaries and intergranular oxidation was also induced, the scale would be composed by particles instead of a continuous layer [19], as it was observed for the steel under examination. Thus, intergranular oxidation does not take place. This conclusion is very important for the resistance of the alloy under question, as this oxidation form could lead to very fast failure of the substrate [11].

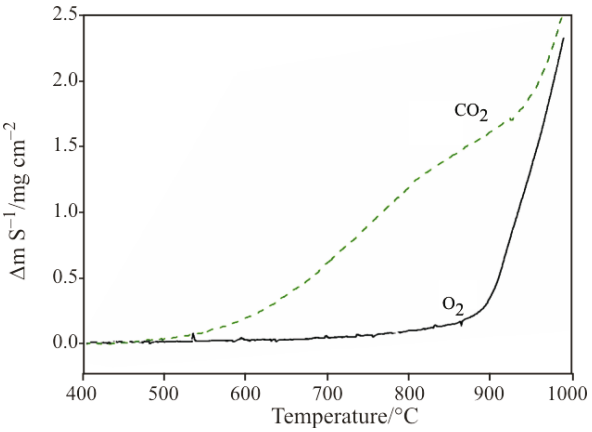

Fig. 6 Thermogravimetric plot of the steel mass change per unit of surface *vs*. temperature in O_2 and CO_2 with heating rate 10°C min^{-1}

Oxidation in CO_2

The plot of Fig. 6 presents the mass change of the examined steel in CO_2 atmosphere. The oxidation in O_2 is also presented for comparison reasons. As it is observed, the mass of the steel increases also in CO_2 atmosphere as the temperature rises. This means that oxidation of the metallic phase takes place.

Nevertheless, the mass change curve is not similar for O_2 and CO_2. As it was already mentioned, in the case of O_2 there is a certain incubation period. During this period the steel surface seems to be rather inert. Nevertheless, at about 900°C a steep increase begins. On the contrary, in the case of CO_2 oxidation begins at a much lower temperature (at about 450°C) and the first steep increase begins at 600°C. In any case, at 1000°C the two curves almost coincide. Consequently, oxidation proceeds in each gas with different mechanism. Furthermore, the existence of a slope change in both curves implies structural or compositional changes in the scale as the temperature rises, which finally result to its failure.

In any case, the plot of Fig. 6 offers an important conclusion useful for technological applications. Since the effect of CO_2 begins at a low temperature, in an atmosphere reach in CO_2 (e.g. exhaust gases) the examined steel would be more vulnerable, as the degradation of the substrate begins much earlier compared to the effect of oxygen.

However, in the case of CO_2 the examination of the oxidation mechanism is rather complicated. CO_2 is able to interact with the substrate carbon. As a result, carburizing (transport of carbon from the gaseous phase to the substrate) or decarburizing (leaching of carbon from steel) is possible following the reaction [9]:

$$C_{(Fe)}+CO_2=2CO$$

Furthermore, CO_2 is also capable to directly oxidize iron following the reactions [11, 20]:

$$Fe+CO_2=FeO+CO$$

$$(1–x)Fe+CO_2=Fe_{1-x}O+CO$$

The interaction mechanism as far as it regards carburizing or decarburizing is mainly affected by the activity of carbon in the substrate and in the environment that is in contact with the substrate. If the activity in the environment is higher than the activity in the metal, carburization occurs, while the opposite phenomenon takes place when the relation between the carbon activities is reverse.

However, as it was already mentioned, CO_2 decomposes whet it is in contact with the substrate. Thus oxygen is also formed, which oxidizes steel. When this phenomenon is fast, a scale is formed on top of the substrate that inhibits the carburizing or decarburizing [11]. As a result, only oxidation takes place.

In our case a similar phenomenon is more likely. As Fig. 7 shows, a thin and compact scale is grown on top of the substrate. On the surface of the scale flakes are distinguished that grow perpendicularly to the steel surface. Their composition shows that they are mainly composed of iron, manganese and oxygen. Similar composition was also observed for the underlying layer of the scale, but in this case the Mn concentration was lower. The lower Mn concentration is in accordance with the observations previously made regarding the oxidation behavior in pure oxygen, where Mn was concentrated close to the scale surface.

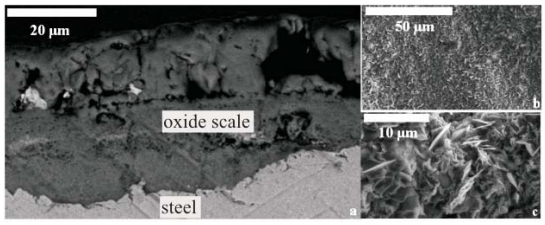

Fig. 7 SEM micrographs of a – the cross-section and b–c – the plane view of oxidized steel after exposure in CO_2 with heating rate 10°C min^{-1}

Conclusions

From the above examination it could be deduced that CO_2 is the most aggressive gas with regard to the examined steel and the examined conditions. Of course this conclusion is valid only for relatively low temperatures because at higher temperatures the effects of CO_2 and O_2 coincide. Under the examined conditions it seems that CO_2 decomposes when it comes in contact with the substrate. Thus, oxygen is formed which oxidizes steel, while the scale formed does not cause carburizing of the steel. In the case of O_2, an oxide scale is formed, which is composed of different Fe, Mn, Mo and Cr oxides adjusted in the form of layers, mainly due to the different diffusion coefficients of each metal in the already formed scale. In any case, the oxidation is uniform, while intergranular oxidation does not take place. Hence the stability of the steel is adequate.

References

1 G. Vourlias, N. Pistofidis, D. Chaliampalias, K. Chrissafis, E. Pavlidou and G. Stergioudis, J. Therm. Anal. Cal., 87 (2007) 401.
2 G. Vourlias, N. Pistofidis, K. Chrissafis and G. Stergioudis, J. Therm. Anal. Cal., 90 (2007) 769.
3 G. Vourlias, N. Pistofidis, E. Pavlidou and K. Chrissafis, J. Therm. Anal. Cal., 90 (2007) 777.
4 R. A. Covert and A. H. Tuthill, Diary, Food Environmental Sanitation, 20 (2000) 506.
5 The International Nickel Company, Standard Wrought Austenitic Stainless Steel, Manual 252, Materials Engineering, 1974.
6 P. Kofstad, High temperature corrosion, Elsevier Applied Science, New York 1988.
7 N. Birks and G. H. Meier, Introduction to High Temperature Oxidation of Metals, Edward Arnold, London 1983.
8 D. W. Rahoi and C. M. Schillmoller, Duplex Stainless Steels for the Chemical, Petroleum and Process Industries, Proceedings of the Annual Materials Engineering Workoshop, Nickel Development Institute, Toronto 1985. pp. 10–13.
9 B. K. Agrawal, Introduction to Engineering Materials, McGraw Hill, New Delhi 1999.
10 M. G. Fontana, Corrosion Engineering, 3rd Ed., McGraw-Hill, New York 1986.
11 J. R. Davis Ed., Heat-Resistant Materials, ASM International, New York 1997.
12 S. H. Park, I. S. Chung and T. W. Kim, Oxid. Met., 49 (1998) 349.
13 H. Hindamm and D. P. Whittle, Oxid. Met., 18 (1982) 245.
14 N. Karimi, F. Riffard, F. Rabaste, S. Perrier, R. Cueff, C. Issartel and H. Buscail, Appl. Surf. Sci., 2007, 10.1016/j.apsusc.2007.09.018.
15 S. K. Putatunda, S. Unni and G. Lawes, Mater. Sci. Eng. A, 406 (2005) 254.
16 CRC Handbook of Physics and Chemistry, 57th Ed., CRC Press, 1976–77.
17 PC Powder Diffraction Files, JCPDS-ICDD, 2000.
18 R. K. Wild, Corr. Sci., 17 (1977) 87.
19 H. Shenk, E. Schmidtman and H. Muller, Arch. Eisenhuttenw., 31 (1960) 121.
20 S. Valette, A. Denoirjean, D. Tetard and P. Lefort, J. All. Comp., 413 (2006) 222.

Received: February 15, 2008
Accepted: September 16, 2008

DOI: 10.1007/s10973-008-9056-5